Zootaxa 5796 (2): 313–331
https://www.mapress.com/zt/

Article

ISSN 1175-5326 (print edition)
ZOOTAXA
ISSN 1175-5334 (online edition)

https://doi.org/10.11646/zootaxa.5796.2.5
http://zoobank.org/urn:lsid:zoobank.org:pub:AF9AC8A0-3015-40D3-9548-1D80E43FD1FF

Morphological and genetic evidence support new species of *Stenocercus* (Iguania: Tropiduridae) from the Peruvian Andes

ERNESTO CASTILLO-URBINA[1,2,3*], SHARY RIOS-ROQUE[1], DIEGO BARRERA-MOSCOSO[1,3] & ALEJANDRO MENDOZA[1,3,]

[1]*Universidad Nacional Mayor de San Marcos, Museo de Historia Natural, Departamento de Herpetología, Av. Arenales 1256, Lima 11, Peru.*
shary49cam@gmail.com; https://orcid.org/0000-0002-0881-6771
[2]*Laboratorio de Sistemática y Ecología de Vertebrados, Facultad de Ciencias Biológicas, UNMSM, Lima, Peru*
[3]*Asociación Ararankha: Ecología y Conservación, Lima, Peru.*
diego.barrera@gmail.com; https://orcid.org/0000-0002-0038-9752
alejandro.mendoza.h13@gmail.com; https://orcid.org/0000-0002-5980-4391
**Corresponding author: ernesto.cas.95@gmail.com; https://orcid.org/0000-0002-8293-758X*

Abstract

The genus *Stenocercus* comprises a diverse group of 80 recognized species distributed across South America, with approximately 65% (52 species) occurring in Peru. The Department of Ancash, situated in the central Andes and encompassing the Cordillera Negra and Cordillera Blanca, is a topographically complex region marked by prominent geographic barriers that may promote allopatric speciation and influence patterns of Andean biodiversity, particularly within *Stenocercus* lineages. Populations previously assigned to *S. chrysopygus* from the puna habitats of Ancash exhibit notable variation in diagnostic traits and coloration, suggesting that this taxon may represent a species complex. However, inconsistent morphological diagnoses and limited genetic data have hindered accurate taxonomic resolution, underscoring the need for integrative approaches. Furthermore, a recent study showed that only populations from the Santa River Valley correspond to *S. chrysopygus* sensu stricto, while the other populations assigned to the distribution of *S. chrysopygus* constitute lineages of different species. In this study, we describe *Stenocercus aguilari* **sp. nov.** from Huari Province, Ancash Department, and present a phylogenetic hypothesis of its position based on the mitochondrial ND2 gene. We applied multivariate morphological analyses of scale counts using MANOVA and Gaussian Mixture Models, as well as molecular species delimitation approaches based on both distance-based and tree-based single-locus methods. All analyses support the taxonomic distinctiveness of *S. aguilari* **sp. nov.** Morphologically, the new species belongs to the group characterized by granular scales on the posterior surface of the thighs, vertebral scales similar in size and shape to adjacent rows, and three caudal whorls per autotomic segment. It is distinguished from other members of this group by the absence of a posthumeral mite pocket, the presence of a Type 1 postfemoral mite pocket, higher number of midbody scales and the presence of a distinct black patch on the pelvic region of the venter in adult males. Finally, the focal lineage is divergent from all nominal species in the *Stenocercus* genus for which respective data are available by >14.8% uncorrected pairwise distance in the ND2 gene.

Key words: Integrative taxonomy, multivariate analysis, molecular species delimitation, Cordillera Blanca

Introduction

Lizards of the genus *Stenocercus* (Iguania: Tropiduridae) comprise a group of 80 species distributed throughout South America, ranging from Ecuador in the north to Argentina in the south, and from Peru in the west to Brazil in the east (Torres-Carvajal 2007a, 2007b; Uetz *et al.* 2025). Of these 80 species, 65% (52 species) are found in Peru. Over the past decade, approximately one new species of *Stenocercus* has been described each year (Venegas *et al.* 2022; Uetz *et al.* 2025), suggesting that several species likely remain undiscovered in poorly explored areas of the Andes.

Accepted by L.J. Avila: 22 Jan. 2026; published: 21 Apr. 2026

One such underexplored region is the Department of Ancash, which encompasses two major Andean ranges: the Cordillera Negra and the Cordillera Blanca. The most recent *Stenocercus* species described from Ancash, *S. johaberfellneri* and *S. amydrorhytus*, were discovered a decade ago in the Cordillera Negra (Köhler & Lehr 2015). To the east lies the Cordillera Blanca, one of the highest mountain ranges in the Andes, with several peaks exceeding 5,000 m a.s.l. This range displays pronounced environmental gradients over short geographic distances, and its uplift, which intensified between ca. 15 and 10 Ma with accelerated surface rise relative to the Cordillera Negra, has played a key role in shaping the evolutionary history of Andean fauna (Velazco & Patterson 2008; Michalak et al. 2015; Grambling et al. 2024). Due to these, the Cordillera Blanca has been proposed to act as a geographic barrier consistent with the orographic vicariance hypothesis, serving as a potential driver of allopatric speciation (Pyron & Burbrink 2010; Pacheco *et al.* 2014; Rengifo & Pacheco 2015). Evidence from birds and mammals supports this idea, with the distribution of some taxa restricted to either the eastern or western slopes of the range, suggesting that the Cordillera Blanca may limit dispersal and promote diversification (Fjeldså & Irestedt 2009; Pacheco *et al.* 2014; Rengifo & Pacheco 2015).

Stenocercus populations found across the highlands of Ancash may have been misidentified as *S. chrysopygus* (Boulenger 1900), a species whose distribution appears to be restricted to the provinces of Recuay and Huaylas between the Cordillera Negra and Cordillera Blanca. Where *S. chrysopygus,* exhibits considerable variation in its diagnostic characters as evidenced by the wide range of scale counts and differences in the coloration pattern between populations from the Pacific and Atlantic basins separated by the Cordillera Blanca (Fritts 1974; Cadle 1998; Torres-Carvajal 2007a). This extensive morphological variation has led to the hypothesis that *S. chrysopygus* may represent a complex of more than one species, and the lack of consistent diagnostic characters and molecular information across all populations in its current range has limited taxonomic resolution (Fritts 1974; Torres-Carvajal 2007a). Previous studies have emphasized the need for more sampling and DNA analysis to adequately assess the taxonomic status throughout its distribution (Torres-Carvajal 2006, 2007b; Texeira *et al.* 2016). Furthermore, a recent study confirmed that the populations assigned to the current distribution of *S. chrysopygus* constitute a species complex, with only the populations in the Santa River valley corresponding to *S. chrysopygus* sensu stricto (Echevarría *et al*. 2025).

In this context of ongoing taxonomic discoveries, we describe a new species of *Stenocercus* collected from the eastern slope of the Cordillera Blanca, Ancash department, based on its morphological and genetic distinctiveness from other *Stenocercus* species. Which was previously identified by Echevarría et al. (2025) as *S. chrysopygus* Clade B.

Materials and methods

Ethics and research. Specimens collected for this study are covered by the following research permits (given by the Ministerio de Agricultura) that include permanent scientific collection of live specimens: RD N° D000074-2023MIDAGRI-SERFOR-DGGSPFFS-DGSPF and RD N° D000039-2023-MIDAGRI-SERFOR-DGGSPFFS-DGSPF.

Field techniques and surveys. Herpetological surveys were conducted in the San Marcos District between 2019 and 2023. Lizards were captured by hand or with the aid of a fishing rod fitted with a slipknot at the tip. Geographic coordinates (expressed in degrees, minutes, and seconds) and elevation were recorded using a Garmin GPS unit (datum: WGS84). All collected specimens were euthanized and fixed in 96% ethanol, then preserved in 70% ethanol for long-term storage. Type specimens are deposited in the herpetological collection of the Museo de Historia Natural, Universidad Nacional Mayor de San Marcos (DH-MUSM) in Lima, Peru.

Species Delimitation. The taxonomic conclusions of this study follow an integrative taxonomy framework for testing species limits (Padial & De la Riva 2010; Padial et al. 2010; Aguilar et al. 2013). Under this approach, we evaluate hypotheses of species boundaries using multiple operational (empirical) criteria or lines of evidence (Leavitt et al. 2015; Aguilar et al. 2016), which represent contingent secondary properties of species (such as monophyly, morphological differentiation, genetic divergence, etc.). Congruence among these independent lines of evidence is taken as strong support for recognizing candidate species as valid, following the general lineage or unified species concept (de Queiroz 2007).

Morphological data. Measurements were taken with digital callipers and recorded to the nearest 0.01 mm. Sex was determined by dissection or by noting the presence or absence of hemipenes. Data on scutellation of

all species of *Stenocercus* compared herein with the new species were from Torres-Carvajal (2007b), Venegas *et al.* (2016), Köhler & Lehr (2015) and Mendoza *et al.* (2021). Specimens reviewed for comparison purposes are listed in Appendix 1. We follow the terminology of Cadle (1991) and Torres-Carvajal (2000, 2007b) for characters included in the description. We estimated egg volume using the elongated spheroid formula employed by Venegas et al. (2022). We followed Pamer et al. (1993), using the term oviductal egg to refer to eggs that had already been released from the ovary and were surrounded by a thin membrane, indicating the early stages of eggshell formation. To ensure accurate comparisons in the present study, we restrict our use of the name *Stenocercus chrysopygus* to individuals collected from its type localities from DH-MUSM collection: Caraz, Huaraz, and Recuay in the Ancash Department, Peru.

To evaluate morphological differentiation between *Stenocercus chrysopygus* and a candidate new species, we analyzed a set of meristic traits (scale counts). Only specimens confidently assigned to *S. chrysopygus* from the type localities and individuals of the putative new species were included in the analyses. For this we tested 6 variables: Scales around midbody, Vertebral scales, Paravertebrals, Gular scales, Fourth finger lamellae, Fourth toe lamellae. All statistical analyses were performed on R v4.4 (R Core Team 2024). We first assessed multicollinearity among variables by calculating Pearson correlation coefficients, and removed one of each pair of variables showing strong correlation ($|r| > 0.9$) (Aguilar *et al.* 2016). To evaluate the assumptions underlying multivariate parametric analyses, we assessed univariate normality within each group using the Shapiro–Wilk test (Shapiro & Wilk 1965), and tested for homogeneity of variances between groups using Levene's test (Levene 1960), both implemented in the *car* package v.3.1-3 (Fox & Weisberg 2019) in R. Additionally, we evaluated multivariate normality using the Henze–Zirkler test (Henze & Zirkler 1990), as implemented in the *mvn* package v.6.1 (Korkmaz *et al.* 2014; version 6.1). To formally test morphological differentiation between *S. chrysopygus* and the candidate species, we performed a Multivariate Analysis of Variance (MANOVA) (Anderson, 2001). This analysis was used to assess whether the two populations differed significantly in multivariate trait space. Finally, to assess whether morphological clusters existed independently of a priori group assignment, we conducted a Gaussian Mixture Model (GMM) clustering analysis using the *mclust* package 6.1.1 in R (Scrucca *et al.* 2016). First, the morphological variables were standardized (z–scores) to eliminate scale differences with the *scale*() function in R. A Principal Component Analysis (PCA) was then performed, and the first two principal components were retained to summarize the major patterns of variation in the dataset. We selected the "VVV" model, which allows ellipsoidal clusters with varying volume, shape, and orientation. The number of clusters was estimated based on the Bayesian Information Criterion (BIC). The optimal number of mixture components was determined using a bootstrap likelihood ratio test (bootstrap LRT), which sequentially compares models with k and k + 1 components. For each comparison, 10,000 bootstrap replicates were generated to assess whether an additional component significantly improved model fit. This probabilistic approach allowed us to evaluate whether the candidate species represents a morphologically discrete cluster.

Genetic data. Our genetic analysis aimed to identify lineage divergence within our focal *Stenocercus* lineage. To ensure representative taxon sampling, we downloaded all available ND2 gene sequences of *Stenocercus* species from GenBank, following Teixeira *et al.* (2016), as listed in Appendix 2. We excluded *S. sinesaccus*, *S. dumerilii*, and *S. albolineatus* due to a high number of ambiguous ("N") sites in their ND2 sequences. *Microlophus koepckeorum* was used as the outgroup. In addition to the new species, we also generated new ND2 sequences for *S. chrysopygus,* which have been deposited in GenBank (Appendix 2). DNA extraction was performed using the Quick–DNA™ extraction kit (Zymo Research), following the manufacturer's protocol. The mitochondrial ND2 gene (NADH dehydrogenase subunit 2) was amplified following the protocols described by Torres-Carvajal (2006), using the primers ND2f.14 (TGACAAAAACTAGCCCC), ND2f.57 (CACAYTTTTGACTNCCAGAAG T), and ND2r.6 (ATTTTTCGTAGTTGGGTTTGRTT). PCR reactions were run with the following thermal profile: an initial denaturation at 95 °C for 30 s, annealing at 46–55 °C for 30 s, and extension at 72 °C for 150 s, repeated for 35 cycles. PCR amplifications were conducted at the Laboratory of Vertebrate Systematics and Ecology, Faculty of Biological Sciences, Universidad Nacional Mayor de San Marcos. PCR products were purified and sequenced by MACROGEN Inc. (Santiago, Chile).

To infer phylogenetic relationships and estimate genetic divergence among *Stenocercus* lineages, we employed both Maximum Likelihood (ML) and Bayesian Inference (BI) phylogenetic approaches. Sequences were exported to AliView v1.26 (Larsson, 2014), manually edited, and aligned using MAFFT v7.310 (Katoh & Standley 2013) with the L–INS–i algorithm as the iterative refinement method (Katoh *et al.* 2005). The final alignment length of the ND2 gene was 1038 bp. We employed IQ–TREE v2.4.0 (Nguyen *et al.* 2015) to infer a molecular phylogeny under

ML as the optimality criterion. Model selection was performed using ModelFinder with the Bayesian Information Criterion (BIC), applied separately to each codon position. The best-fit substitution models were TVM+F+I+G4 for codon position 1, TPM3u+F+I+G4 for codon position 2, and TIM3+F+I+G4 for codon position 3 (using the -m MFP+MERGE command; Kalyaanamoorthy *et al.* 2017). To evaluate branch support, we obtained ultrafast bootstrap values from 2,000 pseudoreplicates, with a maximum of 10,000 unsuccessful iterations before termination (-bb 2000, -nm 10000 in IQ-TREE). We also conducted a Shimodaira–Hasegawa approximate likelihood ratio test (SH-aLRT) with 1,000 replicates (-alrt 1000; Shimodaira & Hasegawa 1999; Guindon *et al.* 2010). Bayesian phylogenetic inference was conducted in MrBayes v3.2.7a (Huelsenbeck & Ronquist 2001; Ronquist *et al.* 2012) under a codon-partitioned model with unlinked substitution parameters across partitions. The dataset was divided into three partitions corresponding to codon positions (1st, 2nd, and 3rd). For each partition, we specified a GTR model (nst=6) with gamma-distributed rate variation among sites (rates=gamma) and fixed the proportion of invariable sites to zero. The prior on rate variation was set to ratepr=variable to allow different evolutionary rates across partitions. Two independent Markov Chain Monte Carlo (MCMC) runs were conducted, each with four chains, for a total of 10 million generations, sampling every 200 generations. Convergence was assessed by checking that the average standard deviation of split frequencies (ASDSF) fell below 0.01 and that the Potential Scale Reduction Factor (PSRF) approached 1.0 across parameters. The outgroup *Microlophus koepckeorum* was specified a priori. A burn-in of 10% was applied, and a majority-rule consensus tree was summarized using the "allcompat" option, retaining bipartitions with a minimum frequency of 0.01 (minpartfreq=0.01). The final tree was visualized using FigTree v1.4.4.

Molecular Species delimitation. To delimit putative species within *Stenocercus*, we implemented both distance-based and tree-based single-locus approaches based on the mitochondrial ND2 gene. We used the same dataset and Bayesian phylogenetic tree previously inferred with MrBayes v3.2.7a (Ronquist *et al.* 2012). As a distance-based method, we used ASAP (Assemble Species by Automatic Partitioning), which detects barcode gaps in pairwise genetic distances to propose species hypotheses (Puillandre *et al.* 2021). The analysis was conducted via the ASAP web server (https://bioinfo.mnhn.fr/abi/public/asap) using the Kimura 2–parameter model, with default parameters and species partitions ranked according to ASAP score. As a tree-based approach, we applied three variants of the Poisson Tree Processes (PTP) method: PTP single rate, mlPTP, and bPTP (Zhang *et al.* 2013; Kapli *et al.* 2017). All analyses were based on the same Bayesian consensus tree. The PTP single rate (p-value=0.001) was run using the mPTP web server (https://mptp.h-its.org/), while mlPTP and bPTP were conducted through the bPTP web server (https://species.h-its.org/), with 100,000 MCMC generations, a thinning interval of 100, and a burn-in of 10% for bPTP. These approaches allowed us to cross-validate species hypotheses using both genetic distance thresholds and phylogenetic branch lengths. Genetic divergence was estimated using pairwise genetic distances (p-distances) calculated in MEGA11 (Tamura *et al.* 2021) under the Kimura 2-parameter model (K2P) (Kimura 1980). Rate variation among sites was modeled using a gamma distribution with a shape parameter of 1. Analyses included all codon positions (1st, 2nd, and 3rd), and ambiguous positions were removed using the pairwise deletion option.

Results

For the morphological analysis, we excluded the Paravertebral variable due to its high correlation with Vertebrals, and also removed the Fourth Finger Lamella variable because it did not meet the assumption of normality. As a result, four variables were retained for the subsequent analyses. We tested for homoscedasticity and multivariate normality, and the MANOVA results supported the existence of two distinct groups ($p < 0.001$). The Wilks' lambda value of 0.10055 indicates that only about 10% of the variance is not explained by the grouping factor. The F-value of 84.983 and the extremely low p-value ($p = 2.2e{-}16$) indicate that the differences between groups are highly significant in multivariate space, considering all four dependent variables simultaneously. The Gaussian Mixture Model (GMM) identified two groups as the most probable clustering solution. All individuals (100%) were correctly assigned to either *S. aguilari* **sp. nov.** or *S. chrysopygus* based on their posterior probabilities. To visualize the clustering, a prediction grid was generated across the PCA space, and the GMM was used to assign each point in this grid to its most probable cluster. This allowed visualization of the classification boundaries. The final PCA plot shows individual data points colored and shaped by their assigned cluster, along with the predicted classification regions, variance is explained at 79.4% by the first two components (Fig. 1).

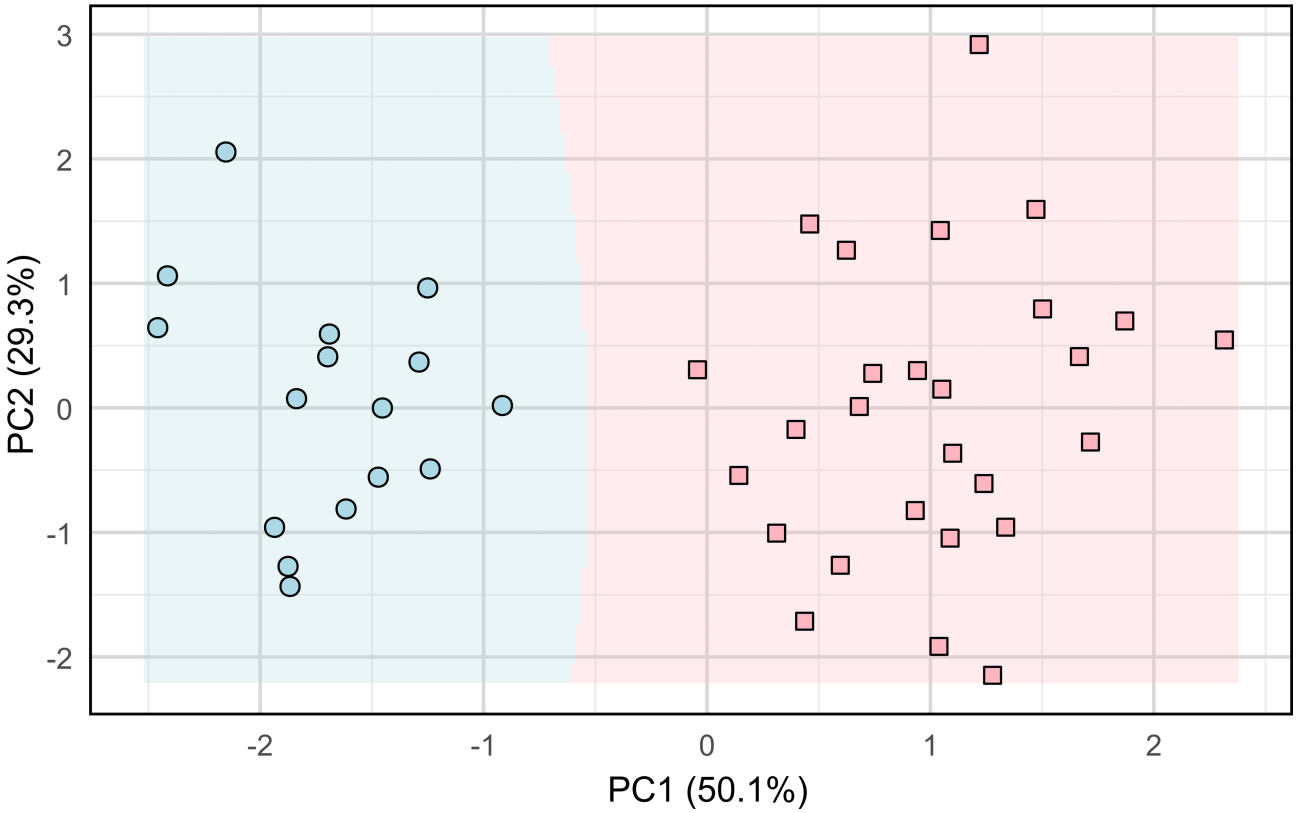

FIGURE 1. Classification plot based on a Gaussian mixture model analysis. All individuals were correctly assigned to their respective clusters. Light blue circles correspond to *S. aguilari* **sp. nov.**, pink-red squares represent specimens of *S. chrysopygus*.

The Bayesian Inference (BI) and Maximum Likelihood (ML) analyses recovered congruent topologies, particularly for branches with high statistical support (Fig. 2). Overall, the BI tree is consistent with previous phylogenetic hypotheses (Torres-Carvajal 2007b; Teixeira *et al.* 2016), recovering Clade A and Clade B as defined by Torres-Carvajal (2007b), although several internal relationships within these clades showed low support values. The newly described species from San Marcos, Ancash, Peru, is nested within Clade A, which predominantly includes species from the central Andes; this clade was recovered with low support in both BI and ML analyses. The two focal specimens formed a strongly supported clade (posterior probability = 1.0; ML bootstrap = 100%; SH–aLRT = 100%) with *S. ornatissimus*, *S. chrysopygus*, *S. latebrosus*, *S. orientalis*, *S. stigmosus*, and *S. melanopygus*. This clade, which contains our focal specimens, is sister to another clade comprising *S. boettgeri*, *S. cupreus*, *S. varius*, *S. empetrus*, *S. eunetopsis*, *S. imitator*, *S. crassicaudatus*, and *S. torquatus*, with *S. humeralis* as the basal lineage to both. This arrangement contrasts with the relationships proposed by Teixeira *et al.* (2016), who recovered *S. humeralis* as sister to *S. varius*. Nevertheless, the relationship between these two clades and *S. humeralis*, within Clade A, was recovered with low support. Clade B was also recovered and placed as sister to Clade A, with strong support (posterior probability = 1.0; ML bootstrap = 99.9%; SH–aLRT = 96%). Uncorrected pairwise genetic distances (ND2) between the new species and its closest relatives within the same clade were as follows: 14.8–15.7% from *S. chrysopygus*, 18.5–18.8% from *S. ornatissimus*, 22.4–22.9% from *S. latebrosus*, 24.8–25.6% from *S. orientalis*, 19.5–20.0% from *S. stigmosus*, and 20.1–20.8% from *S. melanopygus*.

Species delimitation based on molecular data was performed using multiple methods: PTP, bPTP, mlPTP, and ASAP. All approaches consistently supported the distinctiveness of *Stenocercus aguilari* **sp. nov.** and *S. chrysopygus*, clearly separating them from each other and from all other congeners included in the analysis. The ASAP method yielded results congruent with those of the PTP family of models, supporting the same major species boundaries and *S. aguilari* **sp. nov.** and *S. chrysopygus* were always recovered as separate species across all methods. These results reinforce the molecular distinctiveness of *S. aguilari* **sp. nov.** supporting its status as a confirmed undescribed new species.

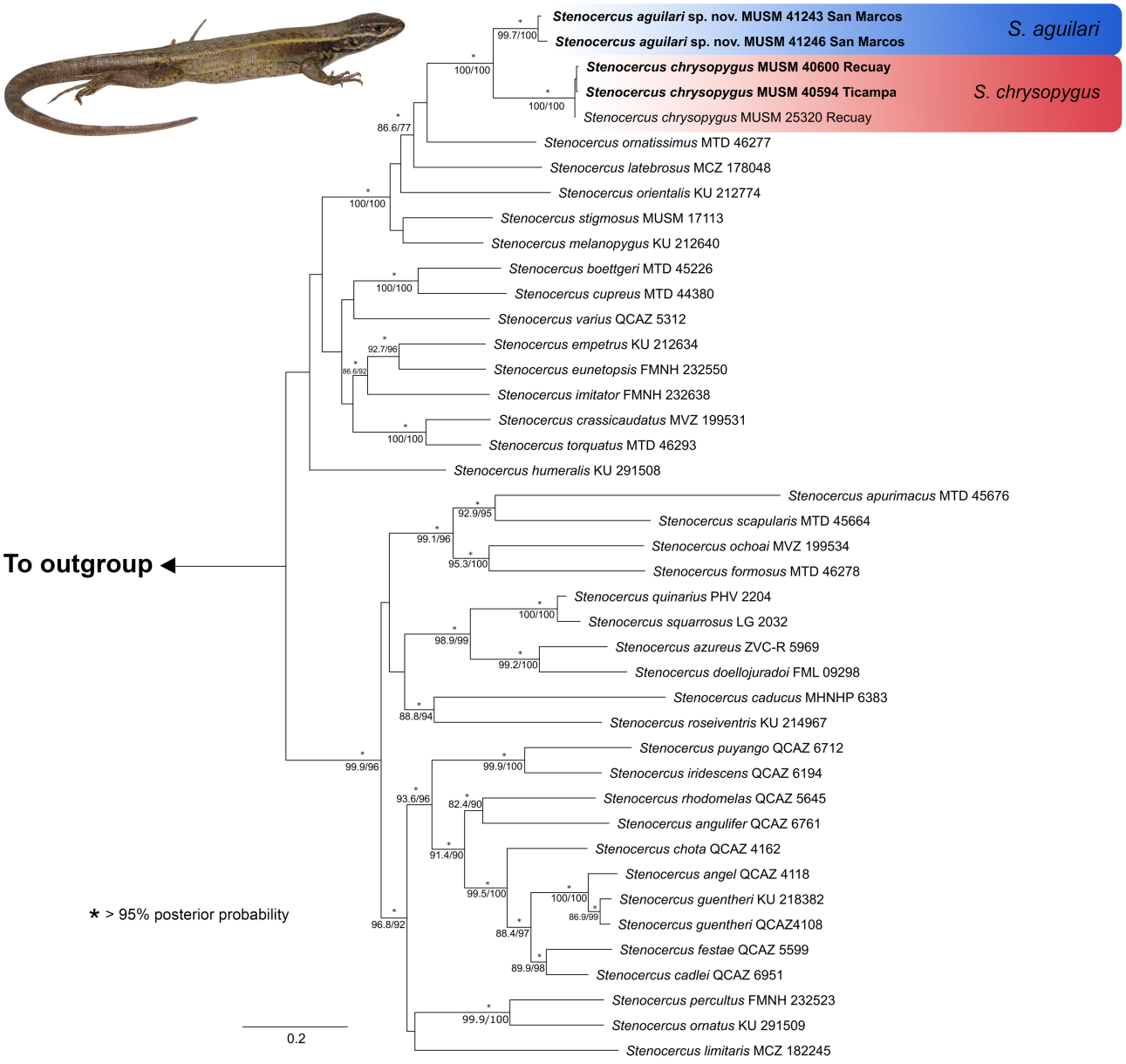

FIGURE 2. Bayesian inference phylogeny of *Stenocercus* based on ND2 sequences (1038 bp). Bold names indicate sequences newly generated in this study. Asterisks (*) on branches denote posterior probabilities ≥ 0.95 from the Bayesian analysis, below support values from the IQ-TREE Maximum Likelihood analysis are shown (ultrafast bootstrap/sh–aLRT support values). Inset photo depicts the holotype of *Stenocercus aguilari* **sp. nov.** (MUSM 41243).

Taxonomy

Stenocercus aguilari **sp. nov.**

urn:lsid:zoobank.org:act:42963394-D25F-46C2-BFD7-5B664A3248FD
Figures 3–6

Stenocercus chrysopygus sensu lato Clade B—Echevarría et. al. (2025)
Stenocercus chrysopygus—Fritts (1974):44

Holotype. MUSM 41243, an adult female, from San Marcos (9°31’6.12”S, 77°7’31.77”W, 3,517 m), Huari Province, Ancash Department, Peru, collected by E. Castillo-Urbina, A. Mendoza and D. Barrera-Moscoso on 20 April 2023.

Paratypes (09): PERU: ANCASH DEPARTMENT: Huari Province: MUSM 41418, adult male, MUSM 41246, MUSM 41039, MUSM 41419, MUSM 41417, MUSM 41244, MUSM 41038, adult females, and MUSM 41245, MUSM 41416, juveniles, from San Marcos (9°31'10.76"S, 77°7'28.68"W, 3,542 m; 9°32'3.81"S, 77° 7'16.36"W, 3,234 m; 9°32'14.98"S, 77°6'41.77"W, 3,334 m), collected by E. Castillo-Urbina, A. Mendoza, V. Herrera and D. Barrera-Moscoso from 2019 to 2023.

Referred specimens (06): PERU: ANCASH DEPARTMENT: Huari Province: MUSM 25326, adult male, MUSM 25321, MUSM 25323, MUSM 25343, adult females, from Chavín de Huántar (9°35'34.56"S, 77°10'34.35"W, 3,158 m), collected by M. Lundberg; PERU: ANCASH DEPARTMENT: Huari Province: MUSM 6958, adult male. MUSM 6955, adult female, from Colcas (9°17'35.94"S, 77°9'24.75"W, 3,481 m), collected by A. Salas.

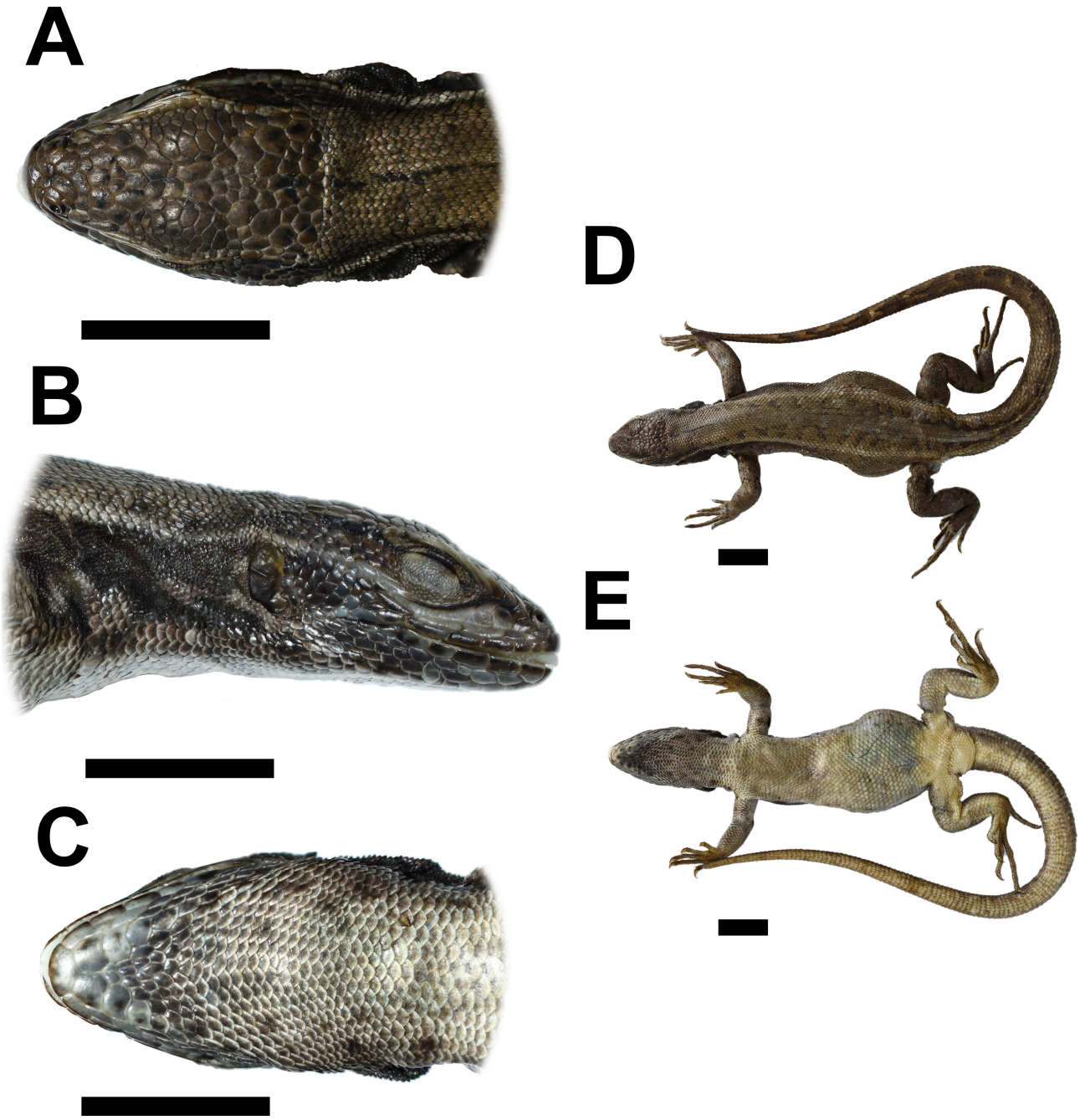

FIGURE 3. *Stenocercus aguilari* **sp. nov.** preserved holotype, adult female, SVL 71.54 mm (MUSM 41243): dorsal (A), lateral (B), and ventral (C) views of the head; dorsal (D) and ventral (E) views of the entire specimen. Photographs by E. Castillo-Urbina. Scale bar = 10 mm.

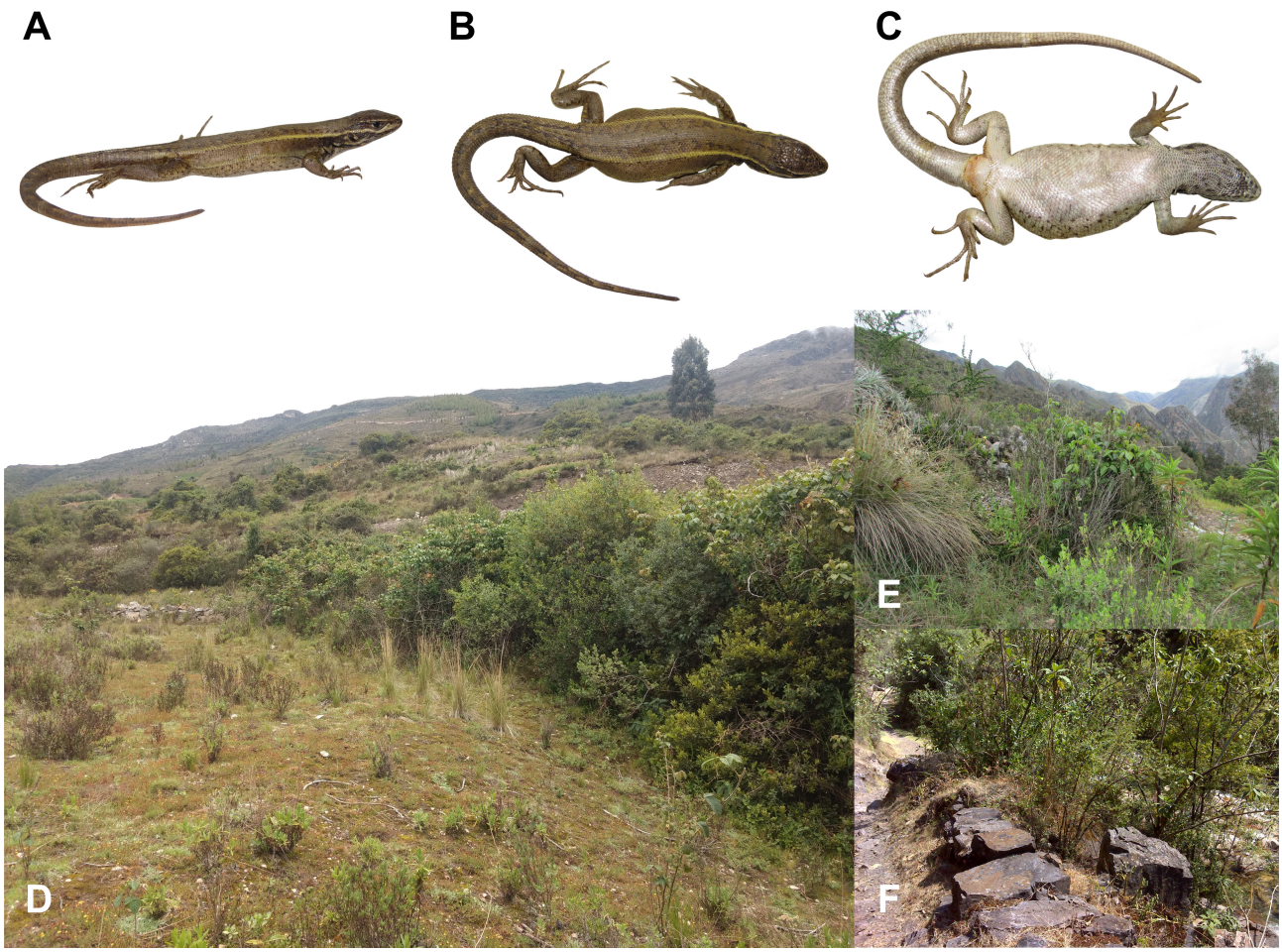

FIGURE 4. (A–C) Lateral, ventral, and dorsal views in life of the adult female holotype of *Stenocercus aguilari* **sp. nov.** (MUSM 41243), SVL 71.5 mm. (D) Panoramic view of the type locality in Ancash, San Marcos. (E–F) Shrubs and rocky microhabitats used for foraging and basking.

Diagnosis. Among the 80 previously known species of *Stenocercus* and the new species described herein, only *S. amydrorhytus*, *S. chrysopygus*, *S. ica*, *S. ivitus*, *S. johaberfellneri*, *S. latebrosus*, *S. melanopygus*, *S. modestus*, *S. omari*, *S. orientalis*, *S. ornatissimus*, and *S. stigmosus* share with *S. aguilari* the combination of granular scales on the posterior surface of the thighs, vertebral scales similar in size and shape to adjacent scale rows, and three caudal whorls per autotomic segment. However, *S. aguilari* is distinguished from all by the combination of lacking a posthumeral mite pocket and possessing a postfemoral mite pocket of Type 1. Moreover, *S. aguilari* differs by having a higher number of midbody scales (65–74 vs. 44–52 in *S. amydrorhytus*, 51–64 in *S. chrysopygus*, 44–48 in *S. ica*, 47 in *S. ivitus*, 47–53 in *S. johaberfellneri*, 43–53 in *S. latebrosus*, 45–59 in *S. melanopygus*, 39–46 in *S. modestus*, 36–47 in *S. omari*, 44–58 in *S. orientalis*, 52–59 in *S. ornatissimus*, and 51–61 in *S. stigmosus*) and more vertebral scales (70–79 vs. 44–52 in *S. amydrorhytus*, 59–68 in *S. chrysopygus*, 44–48 in *S. ica*, 47 in *S. ivitus*, 47–53 in *S. johaberfellneri*, 43–53 in *S. latebrosus*, 45–59 in *S. melanopygus*, 39–46 in *S. modestus*, 36–47 in *S. omari*, 44–58 in *S. orientalis*, 52–59 in *S. ornatissimus*, and 51–61 in *S. stigmosus*). Furthermore, *S. orientalis* and *S. omari* are distinguished from *S. aguilari* (state of character in parentheses) by having strongly keeled dorsal head scales (smooth). Also, *S. ivitus* differs by lacking neck folds (antehumeral, gular, oblique, longitudinal, postauricular, and antegular neck folds present). In addition, *S. aguilari* differs from *S. amydrorhytus*, *S. ica*, and *S. modestus* by having a higher gular scale count (22–28 vs. 18–21 in *S. amydrorhytus*, 15–19 in *S. ica*, and 15–18 in *S. modestus*).

Stenocercus chrysopygus, the sister species of *S. aguilari* **sp. nov.** (state of character between parentheses), differs markedly in a combination of color pattern, scalation, and fold morphology. Males of *S. chrysopygus* show a ventral coloration ranging from orange to pale blue on the lateral margins with a central yellow patch on the pelvic region and thighs (black patch on the pelvic region, Fig. 5). *S. chrysopygus* also exhibits lateral body scales similar

in size to dorsals (smaller than dorsals), and posterior gulars bear an apical notch (no notch). In addition, preserved adult males of *S. chrysopygus* exhibit strongly imbricate, keeled scales along the longitudinal neck fold (weakly imbricate, granular scales, Fig. 6).

Characterization. (1) Maximum SVL in male 76.54 mm (*n* =3); (2) maximum SVL in females 71.54 mm (*n* =13); (3) vertebrals 70–79; (4) paravertebrals 77–85; (5) scales around midbody 65–74; (6) supraoculars 5–7 ; (7) internasals 4; (8) postrostrals 4–6; (9) loreals 1–3; (10) gulars 22–30; (11) lamellae on Finger IV 18–22; (12) lamellae on Toe IV 22–30; (13) posthumeral mite pocket absent; (14) postfemoral mite pocket composed by one or more vertical folds or ridges [Type 1 of Torres-Carvajal (2007b)]; (15) parietal eye present; (16) occipital scales small, smooth, juxtaposed; (17) projecting angulate temporal absent; (18) enlarged supraoculars occupying most of supraocular region in one row absent; (19) scales on frontonasal region smooth, juxtaposed; (20) preauricular fringe present; (21) antehumeral, gular, oblique, longitudinal, postauricular, antegular neck folds present; (22) lateral nuchals smaller than dorsal nuchals; (23) posterior gulars cycloid, smooth, imbricate, apical pit absent; (24) lateral body scales smaller than dorsals body scales; (25) vertebrals similar in size to adjacent dorsals, not forming a continuous longitudinal row; (26) dorsolateral crest absent; (27) ventral scales smooth, imbricate; (28) scales on posterior surface of thighs granular; (29) prefemoral fold absent; (30) inguinal groove absent; (31) preanals not projected; (32) tail not compressed laterally; (33) tail length 60–65% of total length; (34) three caudal whorls per autotomic segment three; (35) caudal not spinose; (36) dark stripe that extends anterodorsally from subocular region to supraciliaries absent; (37) color pattern of gular region in adult females from dark spots to diffuse blotches; (38) color pattern of gular region in adult males with dark spots; (39) black blotch on ventral surface of neck in adult males absent; (40) dark midventral stripe in adult males absent; (41) distinct black patch present on the ventral surface of the thighs, extending along pelvic region of the venter that can extent to the pectoral region in adult males; (42) background color of dorsum grey or brown.

Description of holotype. Adult gravid female (Fig. 3–4); SVL 71.54 mm; TL 107.64 mm (complete); maximum head width 10.92 mm; head length 13.41 mm; head height 8.43 mm; scales on parietal and occipital regions small, slightly wrinkled, juxtaposed; parietal eye visible: supraoculars in six rows, smooth , juxtaposed; circumorbitals present; canthals two; loreals two; postrostrals five; internasals four; supralabials six (right) and seven (left); infralabials seven; lorilabials in one row; preocular single; lateral temporals slightly wrinkled, imbricate; gulars in 26 rows between tympanic openings; all gulars cycloid, smooth, imbricate, apical pit absent; second sublabial in contact with the second and third infralabials; first pair of postmentals in contact medially; mental separated from sublabials by the first pair of postmentals; dorsal scales of neck keeled, imbricate; lateral scales of neck granular, imbricate and the most posteroventral lateral scales of the neck cycloid, smooth and imbricate, lateral scales of body smaller than dorsals, dorsal scales of body keeled, imbricate; the most anterior and posterior lateral scales of body slightly keeled, imbricate, smaller than the most central lateral scales of body keeled, imbricate; scales around midbody 70; vertebrals differentiated from adjacent scales, in 79 rows, not forming a continuous vertebral row; paravertebrals adjacent to vertebral row equal to vertebrals in size and shape; paravertebrals 77; ventrals smooth, imbricate, similar size than dorsals; preauricular fringe present; antegular, oblique, antehumeral, gular, longitudinal and postauricular neck folds present; scales of longitudinal neck fold small, granular, not keeled; ventrolateral fold present; prefemoral fold absent; dorsal scales of forelimbs and hind limbs keeled, imbricate; lamellae on Finger IV 18; lamellae on Toe IV 23 (right) and 22 (left); tail more or less round in cross section; caudals keeled, non-mucronate, imbricate; basal subcaudals smooth, imbricate; posthumeral mite pocket absent; postfemoral mite pocket composed by one or more vertical folds or ridges [Type 1 of Torres-Carvajal (2007b)]

Color in life of holotype: Dorsal head surface brown with black dark flecks. Dorsal body surface grayish brown with paravertebral darkish brown splotches; dorsal surfaces of forelimbs and hindlimbs brownish with darkish brown blotches; dorsal surface of tail grayish brown with darkish brown and light yellowish blotches. Laterally with light yellowish longitudinal stripe from loreal scales to the level of the posterior border of the thighs; lateral surface of head with light yellowish line from canthal scales to superciliar scales; lateral surface of neck blackish dark with light yellowish (stripe from tympanic opening to longitudinal fold) blotches; lateral surface of body with blackish dark speckles and longitudinal pale yellowish stripe; ventrally, with greyish and pale cream scales changes its gular region color from scales greyish with cream borders, gular region with darkish spots; ventral surface of body cream with darkish red splotches. Ventral anal region orangish pale; ventral surface of limbs cream with greyish dark splotches. Iris dark brown.

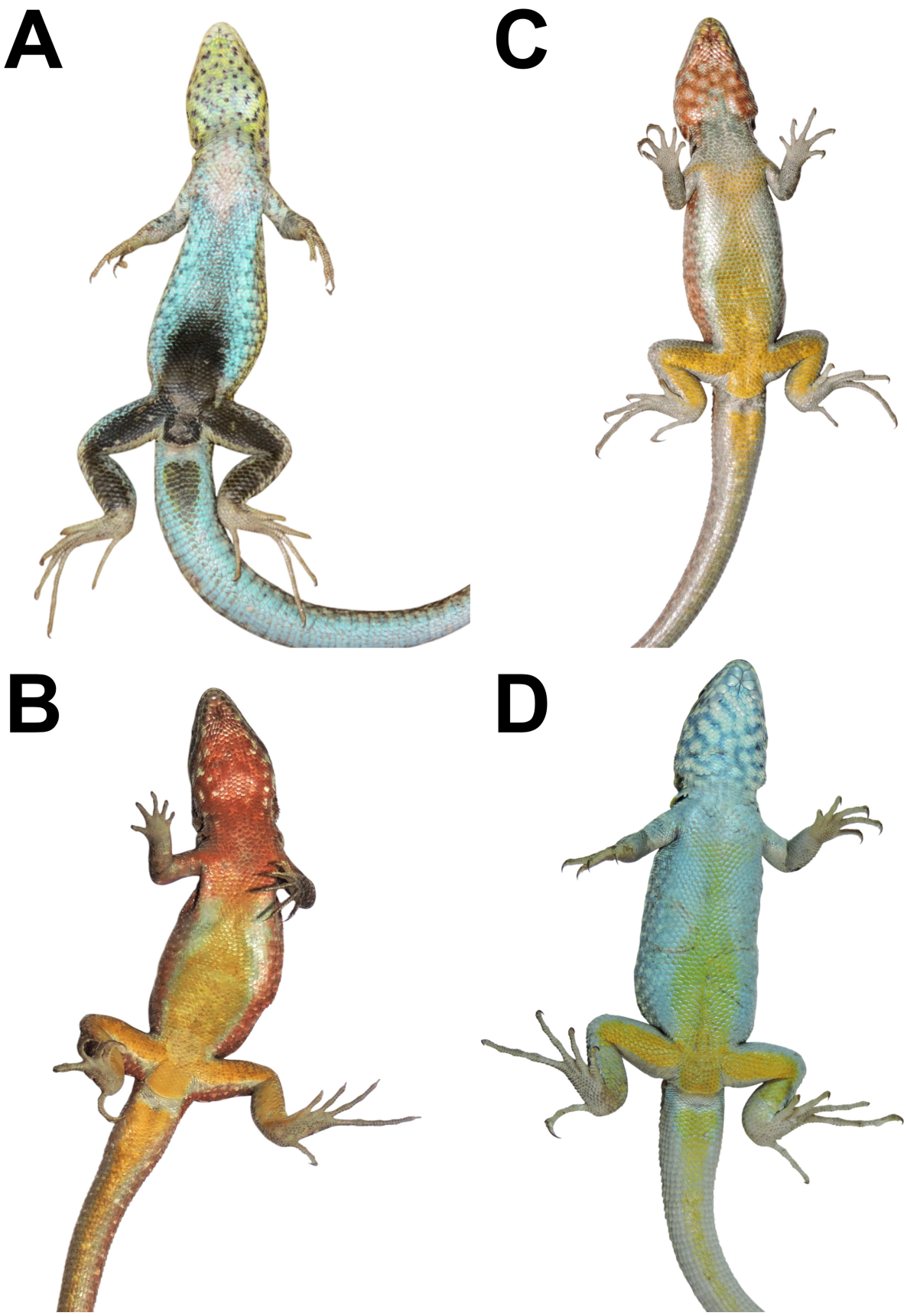

FIGURE 5. Ventral view showing variation in the coloration of adult males of *Stenocercus* in life. (A) *S. aguilari* **sp. nov.** (MUSM 41418), with a distinct black patch on the ventral surfaces the pelvic region, extending along the legs and base of the tail. (B) *S. chrysopygus* (MUSM 39280) from Huaraz. (C) *S. chrysopygus* (MUSM 39301) from Recuay. (D) *S. chrysopygus* (MUSM 39296) from Recuay. Photographs by A. Mendoza and E. Castillo-Urbina.

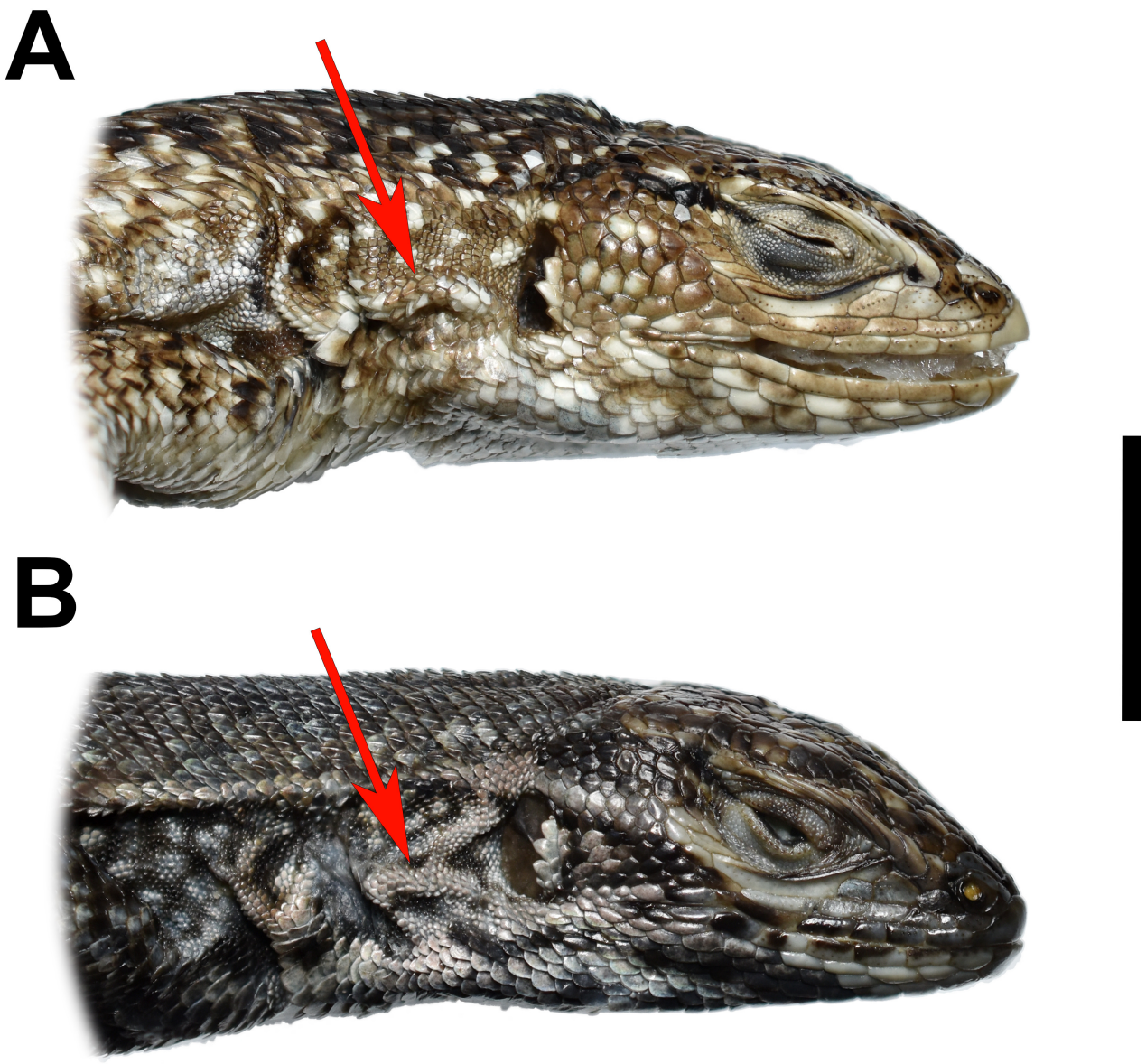

FIGURE 6. Lateral view showing variation in the morphology of the longitudinal neck fold. (A) *S. chrysopygus* (MUSM 40594) from Recuay, adult male, exhibiting strongly imbricate, keeled scales along the longitudinal fold; (B) *S. aguilari* (MUSM 41418), adult male, exhibiting weakly imbricate, granular scales along the longitudinal fold. Photographs by E. Castillo-Urbina. Scale bar = 10 mm.

Intraspecific variation. The paratypes agree with the holotype in morphological characters. Variation in measurements and scutellation of *Stenocercus aguilari* **sp. nov.** are presented in Table 1. Coloration for one male (MUSM 41418) in life was recorded as follows (Fig. 5): dorsal head surface darkish brown with yellowish speckles; dorsal body brownish with scattered yellow scales and mottling of greenish yellow on vertebral region; dorsal surfaces of forelimbs and hindlimbs brownish dark with blotches yellowish and greenish; dorsal surface of tail brownish with scattered yellow and green scales; yellowish vertebral lines up to more than half of the tail; lateral surface of head yellowish and dark brown, lateral surface of neck yellow with darkish brown reticulations; lateral surface of body and tail scattered brown and yellowish scales; pale yellow gular region marked by dark spots, pale blue coloration laterally on the mid and posterior venter, and a distinct black patch on the ventral surfaces of the forelimbs and base of the tail, extending along the mid-posterior region; ventral surface of the hindlimbs pale cream with scattered blue and dark scales. Preserved males from Chavín de Huántar and Colcas also retain the black ventral patch, which persists after many years in preservative. In the male from Chavín de Huántar (MUSM 25326), the black ventral patch extends medially into the pectoral region.

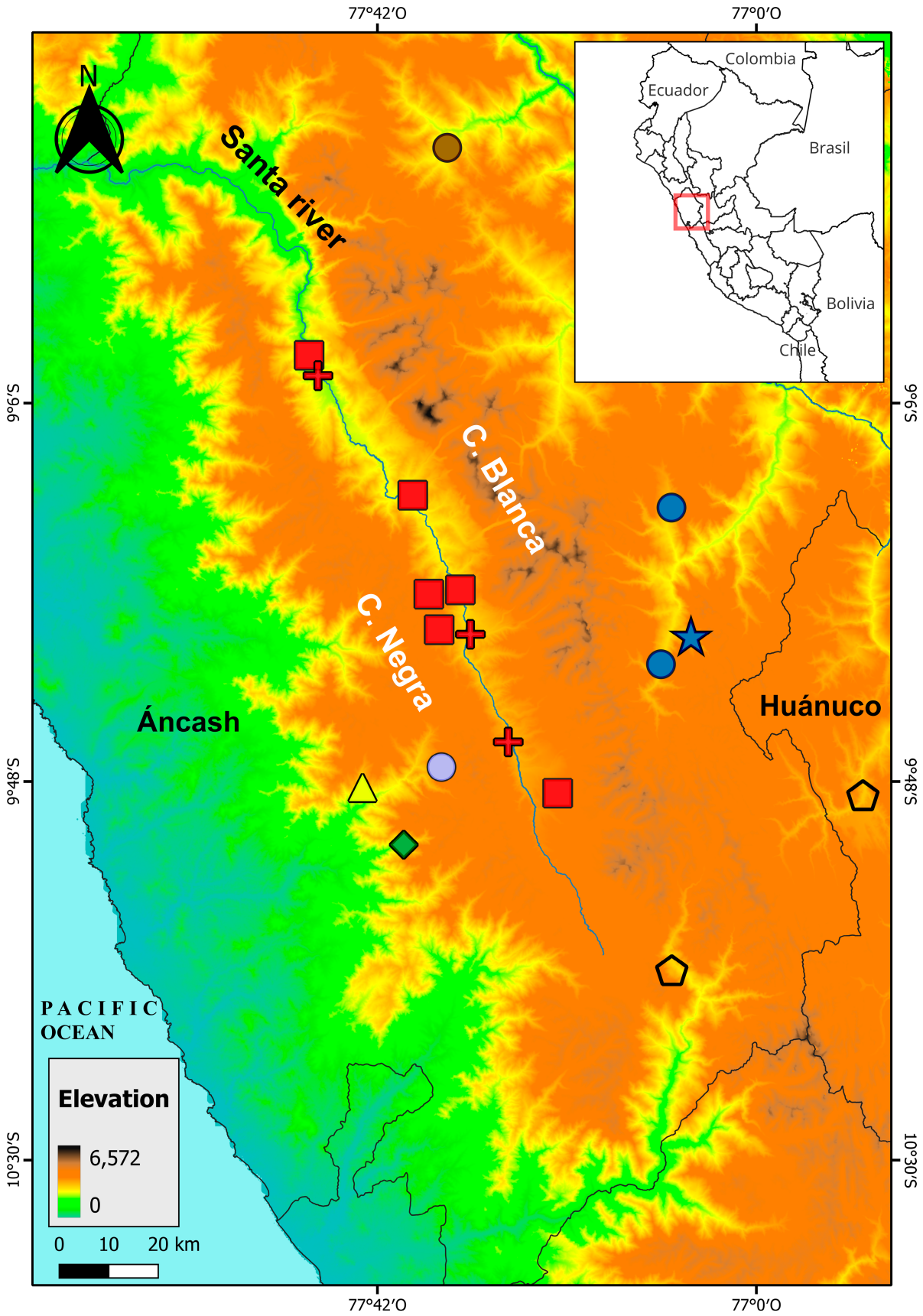

FIGURE 7. Distribution of species of *Stenocercus* in the Ancash region, Peru. Type locality of *S. aguilari* sp. nov. (blue star) and additional records (blue circles); *S. johaberfellneri* (green diamond); *S. amydrorhytus* (yellow triangle); type localities of *S. chrysopygus* (red crosses) and its sensu stricto records (red squares); *S. chrysopygus* sensu lato (Echevarría et al. 2025): Clade C (brown circle) and Clade D (light purple circle); and historical localities of *S. chrysopygus* (pentagons).

TABLE 1. Variation in scutellation and sexual dimorphism in snout-vent length (SVL) of *Stenocercus aguilari* **sp. nov.** and the most morphologically similar species from the western slopes of the Central Andes. Values are presented as ranges followed by means in parentheses. Scale counts and measurements marked with asterisks were taken from Mendoza *et al.* (2021). Mite pocket types follow the classification of Torres-Carvajal (2007b).

Character	*S. amydrorhytus*	*S. chrysopygus*	*S. ica**	*S. johaberfellneri*	*S. modestus**	*S. ornatissimus**	*S. aguilari* **sp. nov.**
	n=7	***n=27***	***n=11***	***n=11***	***n=17***	***n=21***	***n=10***
Maximum SVL males (mm)	68	79	81.5	57	72	66.4	76.54
Maximum SVL females (mm)	60.5	76	62.3	47.5	59	57.4	71.54
Scales around midbody	42–47 (44.3)	51–64 (59.4)	35–38 (37.09)	46–53 (49.2)	35–41 (37.8)	48–59 (53.7)	65–73 (70.2)
Vertebral scales	44–52 (47.3)	59–68 (63.2)	44–48 (46.5)	47–53 (50.0)	39–46 (42.4)	47–61 (53.8)	71–79 (76)
Gular scales	18–21 (19.3)	22–30 (26.4)	15–19 (16.6)	19–24 (21.7)	15–18 (16.5)	20–25 (22.5)	22–28 (26.3)
Internasals	4	2–4	2–4	2–4	2–4	2–6	4
Fourth toe subdigitals	23–26 (24.4)	23–31 (27.4)	28–32 (29.6)	23–27 (24.2)	24–28 (26.2)	22–26 (23.6)	22–27 (25.3)
Tail length / total length	0.61–0.67	0.60–0.69	0.70–0.73	0.62–0.68	0.70–0.73	0.64–0.70	0.60–0.65
Oblique neck fold	Present, covered by imbricate and keeled scales	Present, covered by imbricate and keeled scales	Absent	Present, covered by imbricate and keeled scales	Present, covered by imbricate and keeled scales	Present, covered by imbricate and keeled scales	Present, covered by slightly imbricate and granular scales
posthumeral mite pocket	Type 1	Type 1	Absent	Type 1	Type 1	Type 1	Absent

In females, coloration of the ventral body surface is cream pale with or without dark spots to blotches; ventral surface of thighs and cloaca region is cream pale to orangish yellow; gular region with dark spots to diffuse blotches; dorsal surface of body greyish brown with paravertebral dark blotches and laterodorsal yellowish to pale cream stripe similar to paratype, except in MUSM 41038, which presents pale yellowish spots on dorsal and lateral body, limbs and tail.

Sexual dimorphism in size is evident (Table 1). Adult male is larger and have a more robust head than females. Ventrally, the adult male exhibits a distinct black patch on the belly, forelimbs, and base of the tail, whereas in adult females and juveniles, the belly is pale cream. Dorsally, adult males are brownish with scattered yellow scales, while adult females and juveniles are greyish brown with a laterodorsal stripe ranging from yellowish to pale cream.

Distribution and natural history observations. *Stenocercus aguilari* is currently known from three localities, San Marcos, Chavín de Huantar and Colcas in the eastern sector of the Cordillera Blanca, Ancash Department, Peru, occurring at elevations of 3,158–3,562 m, within the Peruvian Andean steppe ecoregion (Brack & Mendiola 2000).

Individuals of *S. aguilari* were observed during sunny days between 10:00h to 14:00h. Most specimens were found in Andean shrublands or at the edge of stone areas (Fig. 4). When these individuals felt disturbed, they ran quickly into the scrubland finding refuge.

All adult females collected were gravid (SVL = 54.13–71.54 mm). The females were collected in February, April, May, and September. Female MUSM 41244 (SVL = 60.41 mm) had four oviductal eggs (orangish yellow) that were 6.68–7.75 mm wide, 8.51–9.10 mm long, 210.08–368.99 mm^3 of volume. No other lizard species were observed in sympatry.

Etymology. The specific epithet *aguilari* is a patronym honoring Dr. César Aguilar Puntriano, a distinguished Peruvian herpetologist whose contributions have significantly advanced the knowledge and conservation of

Peruvian herpetofauna. His role in strengthening the institutional capacity of the Museo de Historia Natural of the Universidad Nacional Mayor de San Marcos, as both curator and university professor, has been fundamental to the development of herpetology in Peru.

Discussion

After Boulenger (1900) described *Stenocercus chrysopygus* based on three type localities, Caraz, Huaraz, and Recuay, located along the Santa River valley draining into the Pacific Ocean, Fritts (1974) expanded the species distribution to include three additional localities (Fig. 7): Chiquián, extending its range southward to the Chiquián river valley, Chavín de Huantar and La Unión, situated in adjacent inter-Andean valleys draining into the Atlantic basin via the Marañón River. Fritts also noted considerable variation in scale counts and melanistic coloration among males. He interpreted these differences as the result of gradual geographic variation and intraspecific polymorphism, given the ecological similarity among localities. However, the Cordillera Blanca, which separates the Santa valley from the Marañón basin, was not considered as a potential barrier for allopatric speciation. Concordant with Echevarria et al. (2025), we proposed that this mountain range constitutes an allopatric barrier that promoted speciation within the genus *Stenocercus*.

Pronounced differences in male coloration, highlighted by both Fritts (1974) and Torres-Carvajal (2007b), may represent traits under divergent selective pressures or indicators of reproductive isolation in *Stenocercus* as is implied in Venegas *et al.* (2016, 2020, 2022). However, the substantial intraspecific variation observed in species such as *S. chrysopygus*, even within the same population (Fig. 5), indicates that probably this trait should be regarded as a non-definitive diagnostic character. Consistent with our taxonomic decision, males from the Santa River valley exhibit orange to pale blue venters with pale yellow pigmentation on the pelvic region and thighs, whereas, males of *S. aguilari* **sp. nov.** exhibit uniform black coloration on the ventral pelvic region and thighs. Additionally, populations from La Unión and Chiquián were characterized as "markedly melanistic" and given their apparent geographic isolation, these populations may represent divergent lineages and should be evaluated in future studies using integrative data (Fritts 1974; Torres Carvajal 2007b; Echevarría et al. 2025).

A recent study by Echevarría et al. (2025), based on DNA barcoding data sets and morphological data, showed that only the populations of the Santa River valley correspond to *S. chrysopygus* sensu stricto and the other populations assigned to the current distribution of *S. chrysopygus* represents lineages of distinct species, such as the population on the eastern slope of the Cordillera Blanca that here we describe as *S. aguilari*. According to Echevarría et al. (2025), some diagnostic differences between *Stenocercus chrysopygus* and *S. aguilari* (Clade B, Echevarría et al. 2025) are as follows: (1) the presence of a bright yellow patch extending from the lower half of the chest, forming an hourglass shape across the venter and continuing onto the pelvic region, thighs, and shanks in adult males (absent in *S. aguilari*); (2) a reticulated throat pattern in adult males (absent in *S. aguilari*); (3) orange flank coloration (absent in *S. aguilari*); and (4) lateral nuchals less than one-fourth the size of dorsal nuchals, subimbricate, slightly larger, and weakly keeled over the longitudinal, oblique, and antehumeral folds (absent in *S. aguilari*). Our study supports these differences; however, it should be noted that in *S. aguilari* the lateral nuchals are proportionally smaller than the dorsal nuchals, as in *S. chrysopygus*, but they differ by being weakly imbricate, small, and granular over the longitudinal fold (Fig. 6). In addition, our review of populations of *S. chrysopygus* sensu stricto reveals that, besides the reticulated throat pattern, some adult males exhibit a throat with a white spotted pattern, and although the flanks are typically orange, some males display a greenish-yellow flank coloration (Fig. 5). On the other hand, results from our scale count analyses employing Gaussian Mixture Models (GMM) and MANOVA were consistent with those obtained by Echevarría et al. (2025) using the ridgeline manifold method and Discriminant Function Analysis (DFA), all supporting the same morphological gaps and taxonomic differentiation.

The morphological evolutionary hypotheses initially proposed for the genus *Stenocercus* by Etheridge (1970) and Fritts (1974) have been largely supported by subsequent molecular phylogenies (Torres-Carvajal 2006, 2007a; Teixeira *et al.* 2016, Echevarría et al. 2025). These phylogenies, which use multiple mitochondrial markers, including long fragments such as ND1 and ND2, as well as transfer RNAs, have significantly contributed to understanding evolutionary relationships within the group. In line with these findings, this study confirms that the ND2 gene is particularly informative for species delimitation within the genus *Stenocercus*, revealing high levels of genetic divergence among clades. However, a lack of resolution is observed in the basal relationships of the phylogenetic trees, characterized by branches with low support values. This highlights the importance of formulating evolutionary

hypotheses based on molecular data when describing new species, integrating multiple lines of evidence to build a robust taxonomic hypothesis, especially given the limited availability of molecular data for many of the species recently described in Peru (Venegas *et al.* 2013, 2014, 2016, 2020, 2022; Köhler & Lehr 2015; Mendoza *et al.* 2021).

Acknowledgements

This work was made possible through the financial support of Compañía Minera Antamina, as part of its initiative to promote biodiversity research in the Ancash region. The new species of *Stenocercus* was discovered during fieldwork supported by AtkinsRéalis, environmental consultancy firm, responsible for biological monitoring in Antamina. We are grateful to Francesca Montero, Eduardo Almeida, and Claudia Valencia for their technical and logistical assistance during fieldwork and for their comments on an early version of this manuscript. We especially thank Dr. César Aguilar Puntriano for granting permission and providing institutional support to carry out our research at the Museo de Historia Natural San Marcos in the Herpetology Department (DH-MUSM), and the Vertebrate Systematics and Ecology Laboratory (UNMSM). We are grateful to F. Zamora, M. Fernández, L. Echevarría, G. Torres-Ccasani, M. Vargas and V. Herrera for their valuable collaboration during the development of this project.

References

Aguilar, C., Wood Jr, P.L., Cusi, J.C., Guzman, A., Huari, F., Lundberg, M., Mortensen, E., Ramírez, C., Robles, D., Suárez, J., Ticona, A., Vargas, V.J., Venegas, P.J. & Sites Jr, J.W. (2013) Integrative taxonomy and preliminary assessment of species limits in the *Liolaemus walkeri* complex (Squamata, Liolaemidae) with descriptions of three new species from Peru. *ZooKeys*, 364, 47–91.
https://doi.org/10.3897/zookeys.364.6109

Aguilar, C., Wood Jr, P.L., Belk, M.C., Duff, M.H. & Sites Jr, J.W. (2016) Different roads lead to Rome: Integrative taxonomic approaches lead to the discovery of two new lizard lineages in the *Liolaemus montanus* group (Squamata: Liolaemidae). *Biological Journal of the Linnean Society*, 120 (2), 448–467.
https://doi.org/10.1111/bij.12890

Anderson, M.J. (2001) A new method for non-parametric multivariate analysis of variance. *Austral Ecology*, 26 (1), 32–46.
https://doi.org/10.1111/j.1442-9993.2001.01070.pp.x

Boulenger, G.A. (1900) Descriptions of new batrachians and reptiles collected by Mr. P. O. Simons in Peru. *Annals and Magazine of Natural History*, Series 7, 6 (32), 181–186.
https://doi.org/10.1080/00222930008678355

Brack, A. & Mendiola, C. (2000) *Ecología del Perú. Parte II: Las regiones naturales del Perú*. Ediciones Bruño, Lima, Perú, 169 pp.

Cadle, J.E. (1991) Systematics of lizards of the genus *Stenocercus* (Iguania: Tropiduridae) from northern Perú: New species and comments on relationships and distribution patterns. *Proceedings of the Academy of Natural Sciences of Philadelphia*, 143, 1–96.

Cadle, J.E. (1998) New species of lizards, genus *Stenocercus* (Iguania: Tropiduridae), from western Ecuador and Peru. *Bulletin of the Museum of Comparative Zoology*, 155 (6), 257–297.

de Queiroz, K. (2007) Species concepts and species delimitation. *Systematic biology*, 56 (6), 879–886.
https://doi.org/10.1080/10635150701701083

Echevarría, L.Y., Torres-Ccasani, G., Romero, P.E., Torres-Carvajal, O. & Aguilar-Puntriano, C. (2025) Systematics of *Stenocercus chrysopygus* Boulenger, 1900 (Squamata, Tropiduridae) species complex using genetic and morphological evidence. *Zoosystematics and Evolution*, 101 (4), 1747–1762.
https://doi.org/10.3897/zse.101.157306

Etheridge, R. (1970) *Stenocercus*. *In*: Peters, J.A. & Donoso-Barros, R. (Eds.), *Catalogue of Neotropical Squamata. Part II. Lizards and Amphisbaenians*. Smithsonian Institution, Washington D.C., pp. 254–257.

Fjeldså, J. & Irestedt, M. (2009) Diversification of the South American avifauna: Patterns and implications for conservation in the Andes. *Annals of the Missouri Botanical Garden*, 96 (3), 398–409.
https://doi.org/10.3417/2007148

Fox, J. & Weisberg, S. (2019) *An R companion to applied regression* (3rd ed.). Sage Publications.

Fritts, T.H. (1974) A multivariate evolutionary analysis of the Andean iguanid lizards of the genus *Stenocercus*. *San Diego Society of Natural History*, 7, 1–86.

Grambling, T.A., Jessup, M.J., Newell, D.L., Grambling, N.L. & Hiett, C.D. (2024) Magmatic conditions aiding synconvergent extension above the Peruvian flat slab. *Geosphere*, 20 (4), 1102–1132.
https://doi.org/10.1130/GES02741.1

Guindon, S., Dufayard, J.F., Lefort, V., Anisimova, M., Hordijk, W. & Gascuel, O. (2010) New algorithms and methods to estimate maximum-likelihood phylogenies: Assessing the performance of PhyML 3.0. *Systematic Biology*, 59 (3), 307–321.
https://doi.org/10.1093/sysbio/syq010

Henze, N. & Zirkler, B. (1990) A class of invariant consistent tests for multivariate normality. *Communications in Statistics—Theory and Methods*, 19 (10), 3595–3617.
https://doi.org/10.1080/03610929008830400

Huelsenbeck, J.P. & Ronquist, F. (2001) MRBAYES: Bayesian inference of phylogenetic trees. *Bioinformatics*, 17 (8), 754–755.
https://doi.org/10.1093/bioinformatics/17.8.754

Kalyaanamoorthy, S., Minh, B.Q., Wong, T.K.F., Von Haeseler, A. & Jermiin, L.S. (2017) ModelFinder: Fast model selection for accurate phylogenetic estimates. *Nature Methods*, 14 (6), 587–589.
https://doi.org/10.1038/nmeth.4285

Kapli, P., Lutteropp, S., Zhang, J., Kobert, K., Pavlidis, P., Stamatakis, A. & Flouri, T. (2017) Multi-rate Poisson tree processes for single-locus species delimitation under maximum likelihood and Markov chain Monte Carlo. *Bioinformatics*, 33 (11), 1630–1638.
https://doi.org/10.1093/bioinformatics/btx025

Katoh, K. & Standley, D.M. (2013) MAFFT multiple sequence alignment software version 7: Improvements in performance and usability. *Molecular Biology and Evolution*, 30 (4), 772–780.
https://doi.org/10.1093/molbev/mst010

Katoh, K., Kuma, K.I., Toh, H. & Miyata, T. (2005) MAFFT version 5: Improvement in accuracy of multiple sequence alignment. *Nucleic Acids Research*, 33 (2), 511–518.
https://doi.org/10.1093/nar/gki198

Kimura, M. (1980) A simple method for estimating evolutionary rate of base substitutions through comparative studies of nucleotide sequences. *Journal of Molecular Evolution*, 16, 111–120.
https://doi.org/10.1007/BF01731581

Köhler, G. & Lehr, E. (2015) Two new species of lizards of the genus *Stenocercus* (Iguania, Tropiduridae) from central Peru. *Zootaxa*, 3956 (3), 413–427.
https://doi.org/10.11646/zootaxa.3956.3.6

Korkmaz, S., Goksuluk, D. & Zararsiz, G. (2014) MVN: An R package for assessing multivariate normality. *The R Journal*, 6 (2), 151–162. [https://journal.r-project.org/archive/2014-2/korkmaz-goksuluk-zararsiz.pdf]
https://doi.org/10.32614/RJ-2014-031

Larsson, A. (2014) AliView: A fast and lightweight alignment viewer and editor for large datasets. *Bioinformatics*, 30 (22), 3276–3278.
https://doi.org/10.1093/bioinformatics/btu531

Levene, H. (1960) Robust tests for equality of variances. *In*: Olkin I. (Ed.), *Contributions to probability and statistics*. Stanford University Press, Stanford, California, pp. 278–292.

Mendoza, A., Ramírez, C., Barrera, D. & Aguilar-Puntriano, C. (2021) A new species of the genus *Stenocercus* (Iguania: Tropiduridae) from the Peruvian Pacific coast (Ica region). *Salamandra*, 57 (1), 1–14.

Michalak, M.J., Hall, S.R., Farber, D.L., Audin, L. & Hourigan, J.K. (2015) (U-Th)/He thermochronology records late Miocene accelerated cooling in the north-central Peruvian Andes. *Lithosphere*, 8 (2), 103–115.
https://doi.org/10.1130/L485.1

Nguyen, L.T., Schmidt, H.A., Von Haeseler, A. & Minh, B.Q. (2015) IQ-TREE: A fast and effective stochastic algorithm for estimating maximum-likelihood phylogenies. *Molecular Biology and Evolution*, 32 (1), 268–274.
https://doi.org/10.1093/molbev/msu300

Padial, J.M. & De La Riva, I. (2010) A response to recent proposals for integrative taxonomy. *Biological Journal of the Linnean Society*, 101 (3), 747–756.
https://doi.org/10.1111/j.1095-8312.2010.01528.x

Padial, J.M., Miralles, A., De la Riva, I. & Vences, M. (2010) The integrative future of taxonomy. *Frontiers in zoology*, 7 (1), 16.
https://doi.org/10.1186/1742-9994-7-16

Palmer, B.D., Demarco, V.G. & Guillette Jr, L.J. (1993) Oviductal morphology and eggshell formation in the lizard, *Sceloporus woodi*. *Journal of Morphology*, 217 (2), 205–217.

Patterson, B.D. & Velazco, P.M. (2008) Phylogeny of the rodent genus *Isothrix* (Hystricognathi, Echimyidae) and its diversification in Amazonia and the eastern Andes. *Journal of Mammalian Evolution*, 15, 181–201.
https://doi.org/10.1007/s10914-007-9070-6

Puillandre, N., Brouillet, S. & Achaz, G. (2021) ASAP: Assemble species by automatic partitioning. *Molecular Ecology Resources*, 21 (2), 609–620.
https://doi.org/10.1111/1755-0998.13281

Pyron, R.A. & Burbrink, F.T. (2010) Hard and soft allopatry: Physically and ecologically mediated modes of geographic speciation. *Journal of Biogeography*, 37 (10), 2005–2015.

https://doi.org/10.1111/j.1365-2699.2010.02336.x
R Core Team. (2024) R: A language and environment for statistical computing. R Foundation for Statistical Computing. Available from: https://www.r-project.org/ (accessed 27 January 2026)
Rambaut, A., Drummond, A.J., Xie, D., Baele, G. & Suchard, M.A. (2018) Posterior summarization in Bayesian phylogenetics using Tracer 1.7. *Systematic Biology*, 67 (5), 901–904.
https://doi.org/10.1093/sysbio/syy032
Ronquist, F., Teslenko, M., van der Mark, P., Ayres, D.L., Darling, A., Höhna, S., Larget, B., Liu, L., Suchard, M.A. & Huelsenbeck, J.P. (2012) MrBayes 3.2: Efficient Bayesian phylogenetic inference and model choice across a large model space. *Systematic Biology*, 61 (3), 539–542.
https://doi.org/10.1093/sysbio/sys029
Scrucca, L., Fop, M., Murphy, T.B. & Raftery, A.E. (2016) mclust 5: Clustering, classification and density estimation using Gaussian finite mixture models. *The R Journal*, 8 (1), 289–317.
https://doi.org/10.32614/RJ-2016-021
Shapiro, S.S. & Wilk, M.B. (1965) An analysis of variance test for normality (complete samples). *Biometrika*, 52 (3/4), 591–611.
https://doi.org/10.2307/2333709
Shimodaira, H. & Hasegawa, M. (1999) Multiple comparisons of log-likelihoods with applications to phylogenetic inference. *Molecular Biology and Evolution*, 16 (8), 1114–1116.
https://doi.org/10.1093/oxfordjournals.molbev.a026201
Tamura, K., Stecher, G. & Kumar, S. (2021) MEGA11: Molecular Evolutionary Genetics Analysis Version 11. *Molecular Biology and Evolution*, 38 (7), 3022–3027,
https://doi.org/10.1093/molbev/msab120
Teixeira, M.Jr., Prates, I., Nisa, C., Silva-Martins, N.S.C., Strüssmann, C. & Rodrigues, M.T. (2016) Molecular data reveal spatial and temporal patterns of diversification and a cryptic new species of lowland *Stenocercus* Duméril & Bibron, 1837 (Squamata: Tropiduridae). *Molecular Phylogenetics and Evolution*, 94, 410–423.
https://doi.org/10.1016/j.ympev.2015.09.010
Torres-Carvajal, O. (2000) Ecuadorian lizards of the genus *Stenocercus* (Squamata: Tropiduridae). *Scientific Papers, Natural History Museum, The University of Kansas*, 15, 1–38.
https://doi.org/10.5962/bhl.title.16286
Torres-Carvajal, O., Schulte, J.A. & Cadle, J.E. (2006) Phylogenetic relationships of South American lizards of the genus *Stenocercus* (Squamata: Iguania): A new approach using a general mixture model for gene sequence data. *Molecular Phylogenetics and Evolution*, 39 (1), 171–185.
https://doi.org/10.1016/j.ympev.2005.09.007
Torres-Carvajal, O. (2007a) Phylogeny and biogeography of a large radiation of Andean lizards (Iguania, *Stenocercus*). *Zoologica Scripta*, 36 (4), 311–326.
https://doi.org/10.1111/j.1463-6409.2006.00284.x
Torres-Carvajal, O. (2007b) A taxonomic revision of South American *Stenocercus* (Squamata: Iguania) lizards. *Herpetological Monographs*, 21 (1), 76–178.
https://doi.org/10.1655/06-001.1
Uetz, P., Freed, P., Aguilar, R., Reyes, F., Kudera, J. & Hošek, J. (Eds.) (2025) The Reptile Database. Available from: http://www.reptile-database.org (accessed 24 July 2025)
Venegas, P.J., Durán, V. & Garcia-Burneo, K. (2013) A new species of arboreal iguanid lizard, genus *Stenocercus* (Squamata: Iguania), from central Peru. *Zootaxa*, 3609 (3), 291–301.
https://doi.org/10.11646/zootaxa.3609.3.3
Venegas, P.J., Echevarría, L.Y. & Alvarez, S.C. (2014) A new species of spiny-tailed iguanid lizard (Iguania: *Stenocercus*) from northwestern Peru. *Zootaxa*, 3753 (1), 47–58.
https://doi.org/10.11646/zootaxa.3753.1.4
Venegas, P.J., Echevarría, L.Y., García-Burneo, K. & Koch, C. (2016) A new species of iguanid lizard, genus *Stenocercus* (Squamata: Iguania), from the Central Andes in Peru. *Zootaxa*, 4205 (1), 52–64.
https://doi.org/10.11646/zootaxa.4205.1.4
Venegas, P.J., Echevarría, L.Y., García-Ayachi, L.A. & Landauro, C.Z. (2020) Two new sympatric species of *Stenocercus* (Squamata: Iguania) from the inter-Andean valley of the Mantaro River, Peru. *Zootaxa*, 4858 (4), 555–575.
https://doi.org/10.11646/zootaxa.4858.4.5
Venegas, P.J., García-Ayachi, L.A., Chávez-Arribasplata, J.C. & García-Bravo, A. (2022) Four new species of polychromatic spiny-tailed iguanian lizards, genus *Stenocercus* (Iguania: Tropiduridae), from Peru. *Zootaxa*, 5115 (1), 1–28.
https://doi.org/10.11646/zootaxa.5115.1.1
Zhang, J., Kapli, P., Pavlidis, P. & Stamatakis, A. (2013) A general species delimitation method with applications to phylogenetic placements. *Bioinformatics*, 29 (22), 2869–2876.
https://doi.org/10.1093/bioinformatics/btt499

APPENDIX 1

Material examined.

Stenocercus chrysopygus– PERU: Ancash: Recuay: Recuay: MUSM 25320, 39287–39302 (Topotypes), Ancash: Recuay: Ticapampa: MUSM 40591–40595, 40603 (Topotypes), Ancash: Huaraz: Independencia: MUSM 39282–39286 (Topotypes), Ancash: Huaraz: Jangas: MUSM 39303–39304, Ancash: Huaraz: Pira: MUSM 39280 (Topotype), Ancash: Huaraz: Caraz: MUSM: 39275–39279 (Topotypes).

Stenocercus johanbellferneri–PERU: Ancash: Huarmey: MUSM: 20225–20228, 20230 (Paratypes), 20229 (holotype).

Stenocercus amydrorhytus–PERU: Ancash: Aija: Coris: MUSM 20221 (holotype), 20222–20224 (paratype).

APPENDIX 2. GenBank accession numbers for specimens included in the phylogenetic analysis. In bold newly generated sequences.

Species	GenBank code	Voucher	Locality
Microlophus koepckeorum	GQ502766	MCZ R-183606	Peru: Cajamarca: 6 km S Chilete
***Stenocercus aguilari* sp. nov.**	PZ098740	MUSM 41243	Peru: Ancash: Huari: San Marcos
***Stenocercus aguilari* sp. nov.**	PZ098741	MUSM 41246	Peru: Ancash: Huari: San Marcos
Stenocercus angel	DQ080212	QCAZ 4118	Ecuador: Carchi: 8km NE El Angel on road El Angel-Tulcán
Stenocercus angulifer	EF565142	QCAZ 6761	Ecuador: Pastaza Puyo, Hostería Safari
Stenocercus apurimacus	DQ080213	MTD 45676	Peru: Apurimac: Cconoc
Stenocercus azureus	DQ080214	ZVC-R 5969	Uruguay: Rivera: surroundings of Bajada de Pena
Stenocercus boettgeri	DQ080215	MTD 45226	Peru: Pasco: Auquimarca
Stenocercus cadlei	JQ687066	QCAZ 6951	Ecuador:Cotopaxi Ambato: Laguna de Yambo
Stenocercus caducus	DQ080216	MHNHP 6383	Paraguay: Concepción: Parque Nacional San Luis de la Sierra
Stenocercus chota	DQ080217	QCAZ 4162	Ecuador: Imbabura: Salinas
Stenocercus chrysopygus	EF565141	MUSM 25320	Peru: Ancash: Recuay: Recuay
Stenocercus chrysopygus	PZ098743	MUSM 40594	Peru: Ancash: Recuay: Ticampa
Stenocercus chrysopygus	PZ098742	MUSM 40600	Peru: Ancash: Recuay: Recuay
Stenocercus crassicaudatus	AF049866	MVZ 199531	Peru: Cuzco: Machu Pichu Ruins
Stenocercus cupreus	DQ080218	MTD 44380	Peru: Huanuco: W of Ichocán
Stenocercus doellojuradoi	AF528744	FML 09298	Argentina: Salta: Anta: Fina Los Colorados
Stenocercus empetrus	DQ080219	KU 212634	Peru: Cajamarca: Cajamarca
Stenocercus eunetopsis	DQ080220	FMNH 232550	Peru: Cajamarca: ca. 1 km SSW Udima, Río Udima
Stenocercus festae	DQ080221	QCAZ 5599	Ecuador: Azuay: Sigsig
Stenocercus formosus	DQ080238	MTD 46278	Peru: Pasco: María Teresa 19 km on road Oxapampa-Llaupi
Stenocercus guentheri	DQ080223	KU 218382	Ecuador: Pichincha: 20.9 km N Quito
Stenocercus guentheri	JQ687070	QCAZ 4108	Ecuador: Pichincha Lloa
Stenocercus humeralis	DQ080224	KU 291508	Ecuador: Loja: 27 km W Loja on road Loja-Zamora,
Stenocercus imitator	DQ080225	FMNH 232638	Peru: Cajamarca: ca. 1 km SSW Udima, Río Udima
Stenocercus iridescens	DQ080226	QCAZ 6194	Ecuador: Esmeraldas: Tonchigüe

.....continued on the next page

APPENDIX 2. (Continued)

Species	GenBank code	Voucher	Locality
Stenocercus latebrosus	DQ080227	MCZ 178048	Peru: Cajamarca: Quebrada Cachil, 3 km (airline) SW Contumazá
Stenocercus limitaris	DQ080228	MCZ 182245	Peru: Piura: Toronche (ca. 16 km airline SE Ayabaca)
Stenocercus marmoratus	EF565143	MHNC-R 1130	no locality data
Stenocercus melanopygus	DQ080229	KU 212640	Peru: Cajamarca: Cajamarca
Stenocercus ochoai	AF528746	MVZ 199534	Peru: Cuzco: Machu Pichu Ruins
Stenocercus ornatus	DQ080231	KU 291509	Ecuador: Loja: Purununa, slopes of Cerro Colambo
Stenocercus ornatissimus	DQ080240	MTD 46277	Peru: Lima: km 80 carretera central: Chacahuaro
Stenocercus orientalis	DQ080230	KU 212774	Peru: Amazonas: Chachapoyas
Stenocercus percultus	DQ080232	FMNH 232523	Peru: Cajamarca: ca. 1 km NE Monte Seco on road El Chorro-Monte Chico
Stenocercus puyango	DQ080233	QCAZ 6712	Ecuador: El Oro: Puyango
Stenocercus quinarius	KT827780	PHV2204	Brazil: Bahia: EE Serra Geral do Tocantins
Stenocercus rhodomelas	DQ080234	QCAZ 5645	Ecuador: Azuay: Santa Isabel
Stenocercus roseiventris	DQ080235	KU 214967	Peru: Madre de Dios: Cuzco Amazonico
Stenocercus scapularis	DQ080222	MTD 45664	Peru: Junín: Pampa Hermosa
Stenocercus squarrosus	KT827783	LG2032	Brazil: Piaui: Serra das Confusoes
Stenocercus stigmosus	DQ080236	MUSM 17113	Peru: Cajamarca: Pargo, 2–3 km (airline) NW El Pargo,
Stenocercus torquatus	DQ080239	MTD 46293	Peru: Pasco: María Teresa, 19 km on road Oxapampa-Llaupi
Stenocercus varius	DQ080237	QCAZ 5312	Ecuador: Cotopaxi: La Otonga reserve